RSC Advances

ROYAL SOCIETY OF CHEMISTRY

www.rsc.org/advances

Journal Name

ARTICLE TYPE

Cite this: DOI: 10.1039/xxxxxxxxxx

Is MRO¶ Pre-peak Possible in Ionic Liquids without an Aliphatic Chain?[†,‡]

Marco Campetella[a], Serena De Santis[a], Ruggero Caminiti[*,a], Paolo Ballirano[b], Claudia Sadun[a], Luana Tanzi[c] and Lorenzo Gontrani[a]

Received Date
Accepted Date

DOI: 10.1039/xxxxxxxxxx

www.rsc.org/journalname

The combination of amino acids anions with a choline cation gives origin to a new and potentially important class of organic ionic liquids that might represent a viable and bio-compatible alternative with respect to the traditional ones. We present here a combined experimental and theoretical study of the Choline-Proline ionic liquid, using both Large and Small Angle X-Ray Diffraction (WAXS-SAXS) and classical and ab initio molecular dynamics calculations, in which we are able to point out for the first time the existence of a low Q peak in X-Ray patterns in the absence of linear or branched alkyl chains. From the calculations, we can obtain theoretical scattering patterns that reproduces very nicely the experimental spectra in all Q ranges, and from the detailed analysis of the radial distribution functions (RDFs) and hydrogen bond patterns, we can state that very strong ion pairs are established in the liquid and the observed pre-peak can be ascribed to the interactions between atoms belonging to different ion pairs.

Ionic liquids (ILs) have been one of the most investigated research field in material science in the last decades, owing to their outstanding chemical and technological properties[1–7]. An interesting subset of ionic liquids recently prepared[8] is composed of cations or anions derived from biomaterials obtainable from renewable sources, such as amino acids, ammonium, guanidinium, choline. More specifically, the combination of choline with amino-acids anions has been recently exploited to provide ionic liquids very low toxicity to humans[1,5,9] and to the environment, though endowed of very desirable solvent properties, such as the ability of selectively dissolving lignin and cellulose from biomasses[10,11]. Owing to relative novelty of these materials, the literature about their structural properties is still rather scarce and limited to general theoretical studies of choline liquids[12] and to a recently developed force field, in which, though, the systems examined contained aminoacids as anions and the well-studied class of imidazolium as cations[13]; no experimental structural studies exist, to our knowledge. Among all the liquids of this class, we chose to report the results obtained for an interesting system synthesised in our lab (see Supplementary Information), choline-proline (see Fig. 1),

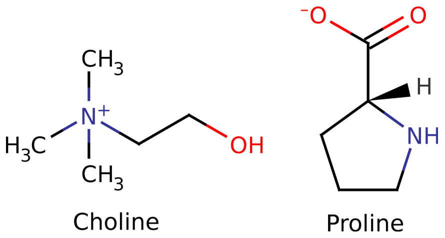

Fig. 1 Representation of Choline cation and Proline anion

since this compound exhibits an unexpected feature, namely the presence of a pre-peak or First Strong Diffraction Peak (FSDP) in the X-Ray scattering patterns collected at small angle (Small Angle X-Ray Scattering, SAXS), *i.e.* a peak falling at shorter Q values than the principal peak of the liquid, analogously of what is generally observed in ionic liquids with medium-long alkyl chains[14,15]. The origin of this feature has been largely debated in several studies[16,17], reaching the generally agreed hypothesis according to which the pre-peak is related to the existence of a medium-range order (MRO), mostly referable to 2nd and higher coordination shells (10 ÷ 20 Å) in the sample[18,19], that

---

[a] *Department of Chemistry, University of Rome "La Sapienza", P.le A. Moro 5, Roma, Italy. Fax: 0039 06490631; E-mail: ruggero.caminiti@uniroma1.it*
[b] *Department of Earth Sciences, University of Rome "La Sapienza", P.le A. Moro 5, Roma, Italy.*
[c] *Department of Physical and Chemical Sciences, University of L'Aquila, Via Vetoio (Coppito 1), 67100 Coppito (AQ), Italy.*

[†] Electronic Supplementary Information (ESI) available: [Experimental procedures and computational details]. See DOI: 10.1039/b000000x/

¶ Medium-Range Order

[‡] These authors contributed equally to this work

in ionic liquids is reflected in the alternation of domains of different polarity[20,21]. Such mesoscopic separation tends to disappear when a polar group is introduced in the alkyl chain[17,22], or when the fragment can undergo some kind of intramolecular interaction that induces a partial folding of the chain[23]. The latter phenomenon could be invoked for proline as well, since the four carbon atoms are arranged in the cycle, thus decreasing the available contact surface for hydrophobic interactions. The absence of well separated domains with cycloalkyl substitution was correlated to some thermodynamic data by our group[24] and was described in a previous structure-activity relationship study by Tao et al[25]. Nevertheless, a clear pre-peak is visible in the small-angle X-Ray scattered intensity (Fig. 2), whose origin is therefore presumably different from the segregation of apolar domains within the charged matrix.

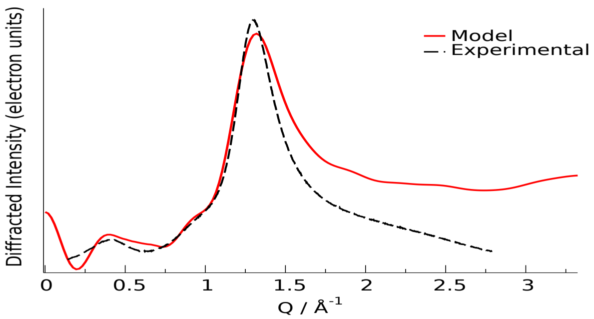

Fig. 2 Small angle X-Ray scattering curve. Experimental: black dash; Model: red line

The first scattering peak of Fig. 2 falls at about 0.4 Å^{-1} and is therefore contributed by medium-range structural correlations in the bulk liquid[18]. The spatial dimension of a suitable interpreting model must therefore be twice as much this value, owing to the Minimum Image Convention of the Periodic Boundary Conditions (PBC) algorithm[26]. Given the large dimension of the system (more than 10K atoms) we decided to perform classical Molecular Dynamics simulations using the GPU-accelerated version of Amber software[27] (see additional material for details), with two-body force field Gaff[28] and properly tuned point charges[29]. The agreement found using this model is very satisfactory in the low Q range of Fig. 2, in particular regarding the position of the peaks. To further assess the model reliability, we confronted the theoretical structural function[30–32], and the relative radial distribution function with the experimental analogues in the medium-long Q range (Wide Angle X-Ray Scattering, WAXS, *i.e.* short distances), and with an alternative higher accuracy theoretical model obtained from first-principle calculations (*ab initio* molecular dynamics)[33]. The scattering function reported in this Q-range (structure function QIQM(Q)) is not suitable to highlight the low-Q peaks contributed by long distance correlations, but is generally preferred when radial patterns descriptive of the system are sought for (See Supp Information, Equation 2). Very good agreements between experimental and calculated patterns (structure factors and radial distribution functions) were found for all Q and r values, see Fig. 3, for both models, though the QM results are clearly superior in all spatial ranges, up their allowed distance limit (half box length).

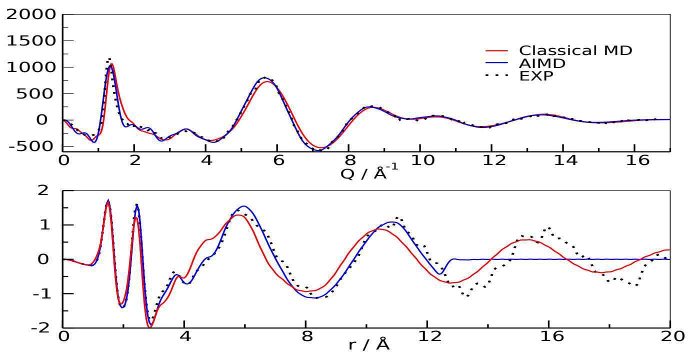

Fig. 3 Structure functions (upper panel) and Radial distribution functions (lower panel). Experimental: black dots; Classical MD: red; AIMD: blue

The quality of the agreement with the experiment made us confident that our calculations were representative of the system, and could be used for further analyses of the microscopic structure of the liquid. One of the most important rheological features of Choline-Aminoacid liquids is the very high viscosity they possess, that can be ascribed to the existence of very strong interactions between the ions. Among all the possible forms of interactions, hydrogen bonds play a major role, as already pointed out in the study of Benedetto et al.[12]. In fact, the relative radial distribution function (between Cho and Pro oxygen atoms), reported in Fig. 4-panel A, shows a sharp peak characterized by the equilibrium distance (2.65 Å and 2.62 Å, for classical and QM models, respectively), significantly shorter than the equilibrium value of 2.75 ÷ 2.8 Å of liquid water[34,35]. This observation suggests that cation and anions give origin to strong ion pairs. To better characterize the cation-anion interaction we have calculated the relative Combined Distribution Function (CDF)[36], that correlates the distance between cation's and anion's oxygen atoms and the distribution of the angle formed by two vectors, the former corresponding to O-H bond and the latter connecting the two hetero atoms; the relative function is shown in Fig. 4-panel B. The region of maximum occurrence in contour plots corresponds to the distance range from 2.5 to 2.9 Å and to the angular interval of 160-180 degrees; these distance and angle values were used as threshold criteria to classify O-H$\cdots$O contacts as hydrogen bonds.[37–39]

The occurrence and time duration of these bonds was derived from a detailed analysis of AIMD trajectory (See Supplementary Information, Computational Details), whose shorter time step and more correct description of the interaction potential was considered more appropriate to investigate the H-bond spatial features and appraise its time evolution. Over a total of 50 ion pairs, we found that 38 cations and 30 anions form persistent bonds during the observed time (35.9 over 40 ps and 38.7 over 40 ps, respectively). The lower number of anions involved is compliant with the presence of two H-bond sites in the carboxylate. To quantify such interaction, we performed an Umbrella Sampling

(U. S.) calculation[40],(See Supplementary Information, Computational Details) on the QM trajectory using the O(Cho)···O(Pro) distance as reaction coordinate; the resulting Potential of Mean Force[41], shown in panel C, has a minimum of about 7 kcal/mol located at 2.62 Å. Such value is similar to the values reported for carboxylic acid dimers in[42–44]and stronger than liquid water (about 5 kcal/mol), in compliance with the shorter O···O distance observed in the radial distribution function.

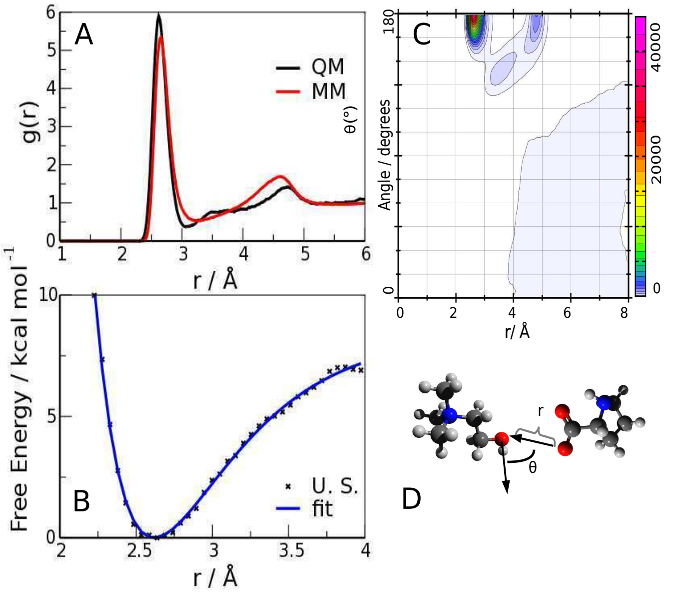

Fig. 4 O(Cho)···O(Pro) Radial distribution function (panel A), Combinated Radial-Angular distribution function (panel B), Free energy profile of H-bond interaction (panel C) and sketch of H-bond (panel D). The blue line is a fit of the free energy data with a Morse-type function

From these results, it can be stated that this pair interaction is largely responsible for the strong structural ordering at low distances; the "structure" of the liquid stems from the packing of the fundamental units, the ion pairs. The overall disposition of the ions, through the interference of their scattered beams, gives origin to the observed spectrum Fig. 3 and 4. The total scattering pattern can be divided into the individual contributions coming from each pair of particles (See Supplementary Information, Equation 3), which can be, in turn, clustered into group terms, like anion and cation. This analysis is reported in Fig. 5, where the whole pattern (black) is decomposed into anion-anion, cation-cation and cation-anion contributions. It can be seen that homologous correlations (cation-cation and anion-anion) lead to the positive peaks at around 0.5 $Å^{-1}$ and are counterbalanced by the intense negative trough due to the mixed cation-anion terms. The resultant curve shows the presence of a pre-peak located around 0.4 $Å^{-1}$ that is also observed in the experimental data. The structural correlations underlying the two peaks can be related to an average "effective distance" of about $2\pi/Q \approx 12.5$ Å, that can be easily appreciated in the g(r)'s between nitrogen and oxygen atoms of cations and anions, respectively, and in their corresponding Fourier-Transform H(Q), the partial contributions to the scattering function (See Supplementary Information, Equation 3) that show a consensus peak at 0.5 $Å^{-1}$. All the curves are reported in Fig. 6, together with the typical geometrical arrangement of particles taken from a trajectory frame, in which the cation-cation contacts are highlighted.

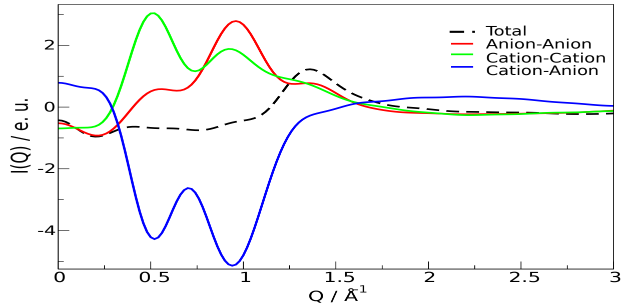

Fig. 5 Individual contributions to low Q diffraction pattern. Black: total; red: cation-cation; green: anion-anion; blue: cation-anion

Summarizing, the results shown indicate that in the Choline-Proline ionic liquid the most important structural feature is the existence of strong ion pairs that mutually solvate one another. The diffraction pre-peak observed can be ascribed to the scattering of second-neighbour groups. In future work, we plan to investigate if this motif can be recognized in other systems lacking hydrophobic moieties, *e.g.* aromatic rings.

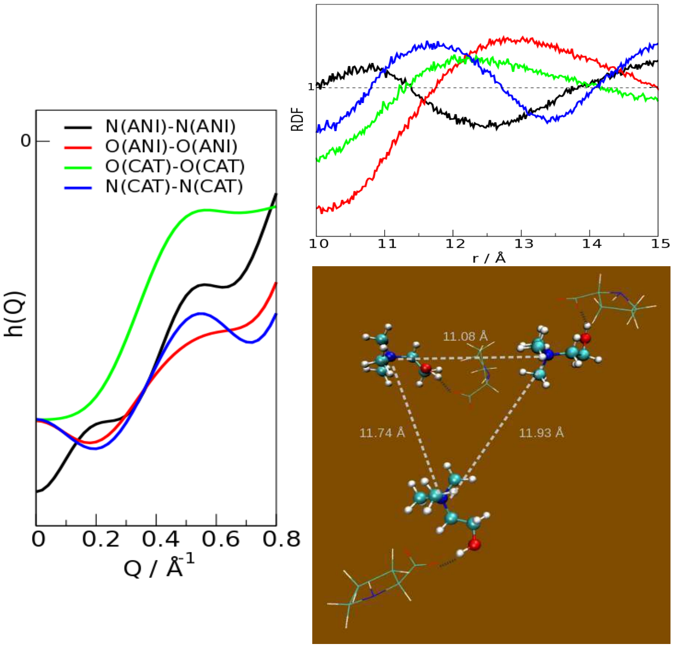

Fig. 6 Partial contributions of heteroatoms. Left: Scattering function H(Q) - Right, top: Radial Distribution Functions - Right, bottom: Typical second-shell arrangement of ion pairs

We are deeply grateful to Enrico Bodo, for his support and for the very helpful discussions. We also thank the Sapienza University of Rome for its Financial Support through grants C26H14P9R2, Prof. Ruggero Caminiti (Sapienza University of

Rome Chemistry Department) for providing free usage of Narten computing cluster facility and Sapienza Nanotechnology Center (CNIS) for providing access to the D8 Diffractometer. Computational support from PRACE (grant n.2013091962) is also acknowledged.

References

1 P. Nockemann, B. Thijs, K. Driesen, C. R. Janssen, K. Van Hecke, L. Van Meervelt, S. Kossmann, B. Kirchner and K. Binnemans, *J. Phys. Chem. B*, 2007, **111**, 5254–5263.

2 Y. Fukaya, Y. Iizuka, K. Sekikawa and H. Ohno, *Green Chem.*, 2007, **9**, 1155–1157.

3 Y. Yu, X. Lu, Q. Zhou, K. Dong, H. Yao and S. Zhang, *Chemistry – A European Journal*, 2008, **14**, 11174–11182.

4 J.-C. Plaquevent, J. Levillain, F. Guillen, C. Malhiac and A.-C. Gaumont, *Chem. Rev.*, 2008, **108**, 5035–5060.

5 M. Petkovic, J. L. Ferguson, H. Q. N. Gunaratne, R. Ferreira, M. C. Leitao, K. R. Seddon, L. P. N. Rebelo and C. S. Pereira, *Green Chem.*, 2010, **12**, 643–649.

6 A. J. L. Costa, M. R. C. Soromenho, K. Shimizu, I. M. Marrucho, J. M. S. S. Esperança, J. N. C. Lopes and L. P. N. Rebelo, *ChemPhysChem*, 2012, **13**, 1902–1909.

7 Y. Gao, S. W. Arritt, B. Twamley and J. M. Shreeve, *Inorg. Chem.*, 2005, **44**, 1704–1712.

8 C. Rüss and B. Konig, *Green Chem.*, 2012, **14**, 2969–2982.

9 K. D. Weaver, H. J. Kim, J. Sun, D. R. MacFarlane and G. D. Elliott, *Green Chem.*, 2010, **12**, 507–513.

10 Q.-P. Liu, X.-D. Hou, N. Li and M.-H. Zong, *Green Chem.*, 2012, **14**, 304–307.

11 X.-D. Hou, T. J. Smith, N. Li and M.-H. Zong, *Biotechnology and Bioengineering*, 2012, **109**, 2484–2493.

12 A. Benedetto, E. Bodo, L. Gontrani, P. Ballone and R. Caminiti, *J. Phys. Chem. B*, 2014, **118**, 2471–2486.

13 V. V. Chaban and E. E. Fileti, *J. Phys. Chem. B*, 2015, **119**, 3824–8.

14 O. Russina, A. Triolo, L. Gontrani and R. Caminiti, *J. Phys. Chem. Lett.*, 2012, **3**, 27–33.

15 M. Campetella, L. Gontrani, F. Leonelli, L. Bencivenni and R. Caminiti, *ChemPhysChem*, 2015, **16**, 197–203.

16 C. Hardacre, J. D. Holbrey, C. L. Mullan, T. G. A. Youngs and D. T. Bowron, *J. Chem. Phys.*, 2010, **133**, 074510.

17 O. Russina, A. Triolo, L. Gontrani, R. Caminiti, D. Xiao, L. G. H. Jr, R. A. Bartsch, E. L. Quitevis, N. Plechkova and K. R. Seddon, *J. Phys. Cond. Matt.*, 2009, **21**, 424121.

18 P. H. Gaskell and D. J. Wallis, *Phys. Rev. Lett.*, 1996, **76**, 66–69.

19 G. Lucovsky and J. C. Phillips, *Phys. Status Solidi B*, 2009, **246**, 1806–1812.

20 H. K. Kashyap, C. S. Santos, R. P. Daly, J. J. Hettige, N. S. Murthy, H. Shirota, E. W. Castner and C. J. Margulis, *J. Phys. Chem. B*, 2013, **117**, 1130–1135.

21 A. Triolo, O. Russina, H.-J. Bleif and E. Di Cola, *J. Phys. Chem. B*, 2007, **111**, 4641–4644.

22 A. Triolo, O. Russina, R. Caminiti, H. Shirota, H. Y. Lee, C. S. Santos, N. S. Murthy and E. W. Castner, Jr, *Chem. Commun.*, 2012, **48**, 4959–4961.

23 M. Campetella, L. Gontrani, E. Bodo, F. Ceccacci, F. C. Marincola and R. Caminiti, *J. Chem. Phys.*, 2013, **138**, 184506.

24 S. De Santis, G. Masci, F. Casciotta, R. Caminiti, E. Scarpellini, M. Campetella and L. Gontrani, *Phys. Chem. Chem. Phys.*, 2015, accepted., n/a.

25 D.-J. Tao, Z. Cheng, F.-F. Chen, Z.-M. Li, N. Hu and X.-S. Chen, *J. Chem. Eng. Data*, 2013, **58**, 1542–1548.

26 M. P. Allen and D. J. Tildesley, *Computer Simulation of Liquids*, Oxford University Press, 1987.

27 A. W. Goetz, M. J. Williamson, X. Dong, Poole, Duncan, Grand, S. Le and W. R. C., *J. Chem. Theory Comput.*, 2012, **8**, 1542–1555.

28 J. Wang, W. Wang, P. A. Kollman and D. A. Case, *J. Mol. Graph. Model.*, 2006, **25**, 247 – 260.

29 Y. Zhang and E. J. Maginn, *J. Phys. Chem. B*, 2012, **116**, 10036–10048.

30 L. Gontrani, O. Russina, F. C. Marincola and R. Caminiti, *J. Chem. Phys.*, 2009, **131**, 244503.

31 V. R. Albertini, L. Bencivenni, R. Caminiti, F. Cilloco and C. Sadun, *J. Macromol. Sci., Part B*, 1996, **35**, 199–213.

32 *The structure of Ionic Liquids*, ed. R. Caminiti and L. Gontrani, Springer, 2014, vol. 193.

33 J. Hutter, M. Iannuzzi, F. Schiffmann and J. VandeVondele, *WIREs Comput Mol Sci*, 2013, n/a.

34 T. Head-Gordon and G. Hura, *Chem. Rev.*, 2002, **102**, 2651–2670.

35 A. K. Soper, *ISRN Physical Chemistry*, 2013, **2013**, 67.

36 M. Brehm and B. Kirchner, *J. Chem. Inf. Mod.*, 2011, **51**, 2007–2023.

37 K. Dong and S. Zhang, *Chemistry - A European Journal*, 2012, **18**, 2748–2761.

38 E. Bodo, A. Sferrazza, R. Caminiti, S. Mangialardo and P. Postorino, *J. Chem. Phys.*, 2013, **139**, 144309.

39 L. Gontrani, E. Bodo, A. Triolo, F. Leonelli, P. D'angelo, V. Migliorati and R. Caminiti, *J. Phys. Chem. B*, 2012, **116**, 13024–13032.

40 G. Torrie and J. Valleau, *J. Comput. Phys.*, 1977, **23**, 187 – 199.

41 S. Kumar, J. M. Rosenberg, D. Bouzida, R. H. Swendsen and P. A. Kollman, *J. Comput. Chem.*, 1995, **16**, 1339–1350.

42 T. Neuheuser, B. A. Hess, C. Reutel and E. Weber, *J. Phys. Chem.*, 1994, **98**, 6459–6467.

43 Y. Gu, T. Kar and S. Scheiner, *J. Am. Chem. Soc.*, 1999, **121**, 9411–9422.

44 M. W. Feyereisen and D. F. andD. A. Dixon, *J. Phys. Chem.*, 1996, **100**, 2993–2997.